Progress In Electromagnetics Research M, Vol. 105, 131–140, 2021

A Wideband Circular Patch Antenna with Pattern Diversity and Reduced Sidelobes

Sai Radavaram and Maria Pour*

Abstract—A wideband circular patch antenna with broadside and conical radiation patterns is proposed. In addition to realizing a wide shared impedance bandwidth of $\sim 48\%$ for both the modes of operation, the unparalleled advantage of the proposed antenna is its reduced sidelobes in the E-plane broadside radiation patterns. The achieved sidelobe-free bandwidth is in the order of 39%, which is much wider than the pertinent art works on wideband pattern diversity antennas using a single radiating patch. The antenna characteristics are validated by fabricating and testing the designed prototype. The proposed antenna is also numerically investigated in front of a parabolic reflector antenna for monopulse radar applications.

1. INTRODUCTION

Pattern diversity antennas with broadside and conical radiation patterns have received significant attention in the recent times owing to their ability to improve the channel efficiency in MIMO wireless communication systems [1] as well as range and angle measurements in monopulse tracking applications [2]. Such reconfigurable radiation pattern antennas operating at a single resonating frequency were reported in [3–6]. Emerging wireless technologies necessitate patch antennas with wideband pattern diversity characteristics. To this end, in [7–10], antennas with wide bandwidth ranges nearing 60% were proposed. However, all these designs consisted of multiple radiating structures, e.g., monopole antennas integrated with the radiating patches in multi-layered structures. The overall thickness of these antennas was greater than $0.15\lambda_o$, where λ_o is the free space wavelength at the center frequency of operation. Moreover, in [7], despite its wide shared impedance bandwidth of $\sim 50\%$, the 3-dB gain bandwidth was only in the order of 33%. By exciting the higher order conical modes in addition to the dominant mode in a single radiating patch, antennas with reconfigurable radiation patterns and wide impedance bandwidth characteristics in the order of 45% were reported in [11–19]. This method reduces the overall volume of the antenna as well as eases the fabrication cost and difficulty. However, the major drawback with all these aforementioned designs is the presence of sidelobes in the E-plane radiation patterns due to the excitation of the next higher order broadside mode in addition to the dominant mode, thus restraining their usage in high gain reflector antennas for monopulse radar applications.

In this article, the unwanted E-plane sidelobes in the radiation patterns are addressed to a large extent in a wideband V-slotted circular patch antenna with pattern diversity characteristics. The radiation pattern reconfigurability is achieved by feeding the antenna with two symmetrically-placed T-shaped probes of equal magnitudes and out-of- and in-phase excitations to realize symmetrical broadside and conical radiation patterns, respectively. The shared impedance bandwidth for both the broadside and conical modes is in the order of 48%, from 3.5 to 5.7 GHz. Moreover, the realized bandwidth range

Received 27 August 2021, Accepted 17 October 2021, Scheduled 20 October 2021
* Corresponding author: Maria Pour (maria.pour@uah.edu).
The authors are with the Department of Electrical and Computer Engineering, The University of Alabama Huntsville, Huntsville, AL 35899, USA.

with no sidelobe levels (SLLs) is about 39% from 3.5 to 5.2 GHz, which is impressively much wider than its counterparts in [12–19]. The antenna is fabricated and its characteristics are measured for validation. The high gain characteristics of the proposed antenna are also numerically studied by placing it at the focal point of an electrically-large parabolic reflector antenna.

2. ANTENNA DESIGN

In the multi-port structures [11–19], to realize pattern diversity, the lateral dimensions of the patch antenna were increased to potentially support the next higher order conical mode along with the dominant mode with broadside radiation patterns. In addition, to improve the impedance bandwidth and the isolation between the ports, different methods were adopted such as slots, proximity feeding techniques, shorting posts, metasurfaces, to name a few [8–19]. Etched slots further increase the overall electrical size of the patch antenna and thereby support the excitation of next higher order broadside mode that inherently contains sidelobes in the E-plane patterns. Shorting posts or vias, on the other hand, push the antenna to resonate at higher frequencies. Therefore, to mitigate the E-plane sidelobes, the lateral dimensions of the patch are to be constrained to cut off the unwanted modes. Moreover, the shape and dimensions of the slots etched on the patch have to be optimized so as to push the resonances of the antenna towards the lower operating frequencies away from the unwanted higher order modes.

Herein, the excitation of the higher order broadside TM_{12} mode is avoided to a larger extent by constraining the radius of the circular patch to $\sim 0.39\lambda_o$ at the center frequency of operation. To utilize the effective area of the patch, two inverted V-shaped slots inspired by [19–24] are then added to the patch that can potentially support both the dominant TM_{11} and conical TM_{21} modes, as shown in Fig. 1. By varying the length l_s and the angle α of the slot-arms, the slots are stretched along the patch so as to enclose a majority of the surface currents. The V-slotted radiating patch is then positioned on the top layer of a 0.5 mm-thick dielectric substrate Rogers RT/duroid 5880LZ ($\varepsilon_r = 1.96$) with the radius $r_g = 66$ mm, close to $1\lambda_o$ near 4.6 GHz. This substrate is separated from another

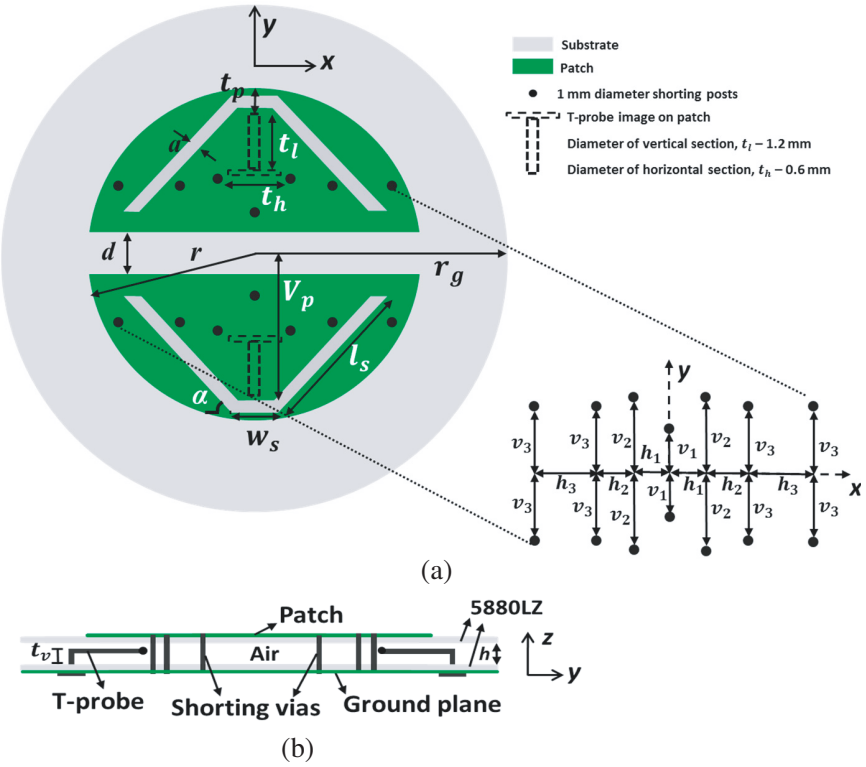

Figure 1. Geometry of proposed antenna. (a) Top view. (b) Cross-sectional view.

grounded substrate with the same dielectric and geometrical properties at a distance of $h = 5.5\,\text{mm}$, $\sim 0.08\lambda_o$, as shown in Fig. 1. As observed, two T-shaped probes are employed to widen the impedance bandwidth and 14 metallic shorting posts are placed at appropriate positions on the patch to improve the isolation between the probes. Dimensions and position of the V-slots, T-shaped probes, and the shorting posts are optimized numerically using the finite-element based EM solver, High Frequency Structure Simulator [25]. The final parameters with which a wide active impedance bandwidth of $\sim 48\%$ is obtained are listed in Table 1.

Table 1. Dimensions of antenna parameters.

Parameter	l_s	w_s	a	d	V_p	α	t_p	t_l	t_h	t_v	v_1	v_2	v_3	h_1	h_2	h_3	h	r
Value (mm)	21.1	11	0.5	7	24	52°	2.4	10	8	4	8	11	10	6	7	8.5	5.5	26

3. NUMERICAL INVESTIGATION

The impact of V-slot parameters on the passive impedance bandwidth characteristics is more or less similar to that of the well-known U-shaped slots, whose results have already been discussed in [26–28], and thus are not repeated here for brevity. To improve the active impedance bandwidth range, shorting posts with a diameter of 1 mm extending from the radiating patch to the ground plane were initially

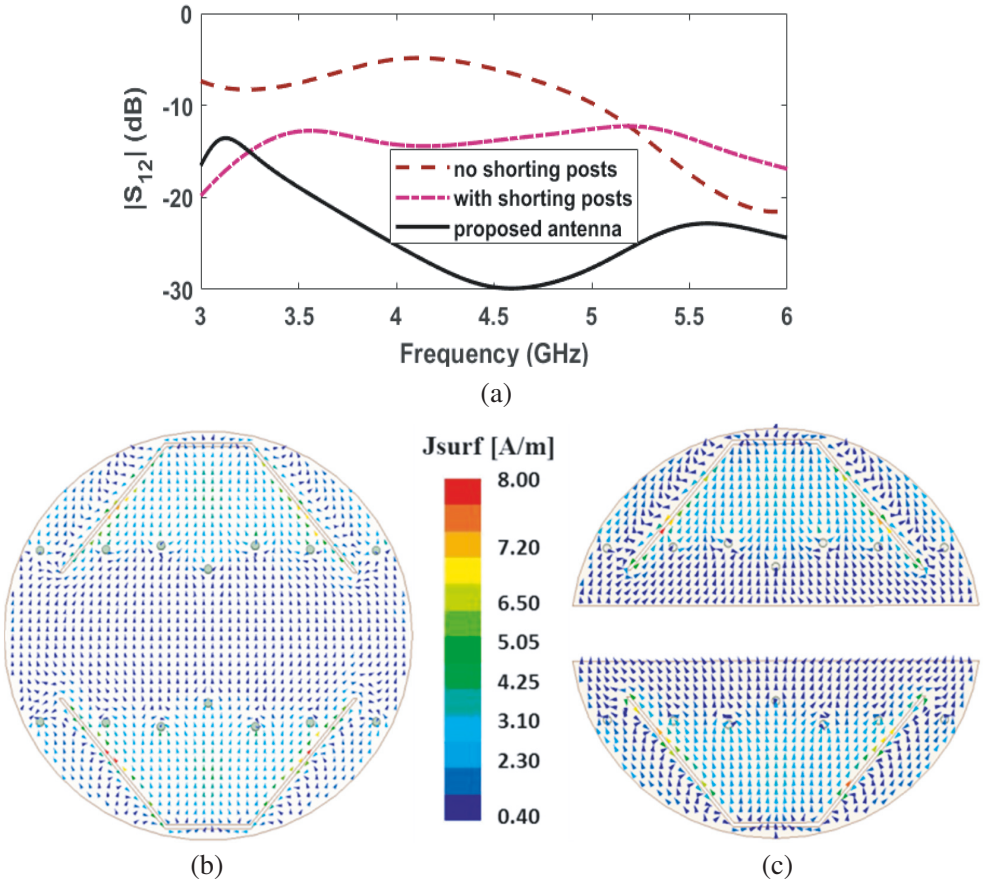

Figure 2. (a) Mutual coupling between the probes without and with the shorting posts and the center gap. (b) & (c) Surface current distributions on the patch when excited in broadside mode at the center frequency of 4.6 GHz, (b) without and (c) with the center gap of width d.

added to the patch at appropriate positions, per Fig. 1. These shorting posts improved the isolation between the closely-spaced probes from 6 dB to better than 10 dB, as depicted in Fig. 2(a). Later, a gap with the width d is formed at the center of the patch, as shown in Fig. 1(a). This gap isolated the upper and the lower halves of the patch, disturbing the continuous distribution of the surface currents on the patch, as illustrated in Figs. 2(b) and 2(c). Such discontinuity of currents aided in further suppression of the mutual coupling between the ports. The realized isolation is better than 20 dB over the entire operating frequency range when $d = 7$ mm. The lower values of d compromise the isolation, whereas its larger values not only diminish the passive reflection coefficient but also degrade the overall antenna gain.

In the proposed antenna, two symmetrically-placed T-shaped probes are used in lieu of widely used L-probes to achieve the radiation pattern reconfigurability with reduced SLLs over a wide impedance bandwidth range. This is better explained by comparing the antenna characteristics of both the L- and T-shaped probes. As per the S-parameters in Fig. 3(a), in both the cases, the isolation between the probes is better than 15 dB over the entire operating frequency range, required for a good active impedance matching. However, the passive S_{11} of the L-probe fed antenna is above the -10 dB level, resulting in a poor shared active impedance bandwidth. The impedance matching can be improved by increasing the length of the horizontal arm of the L-probe, which requires the spreading of shorting posts along the radii of the patch. As such, a larger patch would be needed. This will in turn excite the unwanted higher order broadside modes with the E-plane sidelobes, as shown in Fig. 3(b).

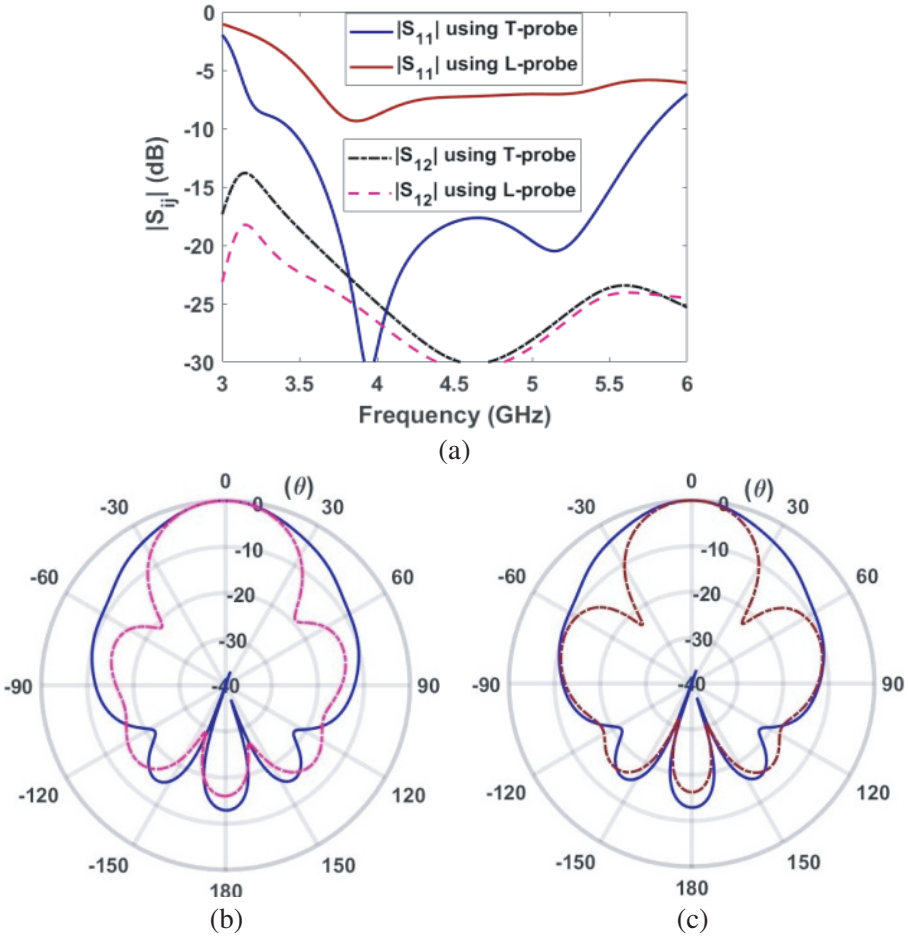

Figure 3. S-parameters of the T-probe and L-probe fed V-slotted circular patch antennas. (b), (c) Simulated E-plane broadside patterns at 4.5 GHz: (b) T-probe vs enlarged L-probe fed patch antenna, (c) T-probe vs L-probe fed antenna with six additional shorting posts; (b), (c) (T-probe; enlarged L-probe; additional shorting posts).

Another approach to improve the matching is by appending additional shorting posts to the patch. Again, this is not preferred as it would further push up the operating frequency range of the antenna, increasing the unwanted sidelobes. To showcase this, six other metallic posts in addition to the actual number of shorting posts used in Fig. 1 were added at appropriate positions on the L-probe fed radiating patch. With proper optimization, a wide shared active impedance bandwidth is realized, however, because of these additional shorting posts, the presence of sidelobes were still very prominent in the E-plane, as shown in Fig. 3(c). To overcome this, the T-shaped probes are employed, introducing additional degrees of freedom through the added T-head section. By finalizing its dimensions, a wide passive reflection coefficient ranging from 3.45 GHz to 5.8 GHz is realized without having to increase the radius of the patch, as shown in Fig. 3(a). Moreover, as opposed to shorting posts, these T-probes have no physical contact with the radiating patch of the antenna and thus they do not change the overall electrical size of the patch, resulting in sidelobe-free patterns, shown by solid curves in Figs. 3(b) and 3(c).

4. ANTENNA CHARACTERISTICS

As shown in Fig. 3(a), the realized passive impedance bandwidth of the proposed antenna with the T-probes is relatively wide covering the 3.45–5.8 GHz range. Moreover, the isolation between the probes is better than 20 dB over the operating frequency range. This improved isolation along with the wide passive reflection coefficient resulted in a wide shared active impedance bandwidth of $\sim 48\%$ from 3.5 to 5.7 GHz, as per Fig. 4, for both the common- (S_{cc11}) and the differential-modes (S_{dd11}), which are expressed by

$$S_{dd11} = S_{11} - S_{12} \tag{1}$$

$$S_{cc11} = S_{11} + S_{12} \tag{2}$$

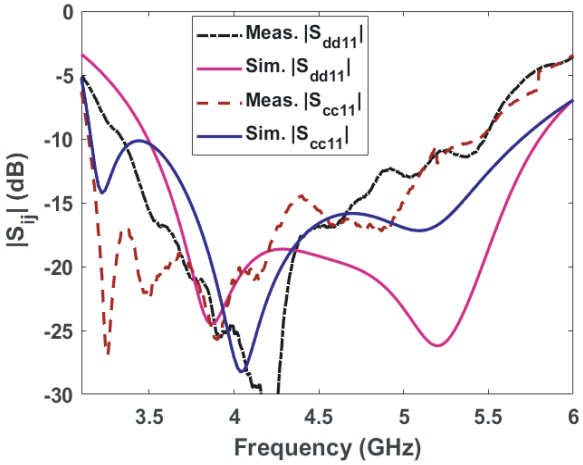

Figure 4. Simulated and measured active reflection coefficients of the proposed antenna.

These simulated results are further validated in practice and the corresponding measured data are overlaid in Fig. 4. The measured active impedance bandwidth range is around 48% over 3.35–5.5 GHz range, thus complying well with the numerical results.

Compared to the antennas in [9–19], the unparalleled advantage of the proposed antenna is its reduced sidelobes in the E-plane when excited in the SUM mode (phase shift between the probes is 180°). To illustrate this, the normalized simulated and measured co- and cross-pol patterns of the antenna in both the E- and H-planes are plotted in Fig. 5 at the frequencies of 3.5, 4, 4.6, 5.1 and 5.7 GHz, exhibiting good agreement between them, where the cross-pol levels are below -20 dB over the entire frequency range. As observed, with the proposed V-slotted circular patch antenna, radiation patterns with no SLLs are obtained over the frequency range of 3.5–5.2 GHz, thus realizing a SLL-free

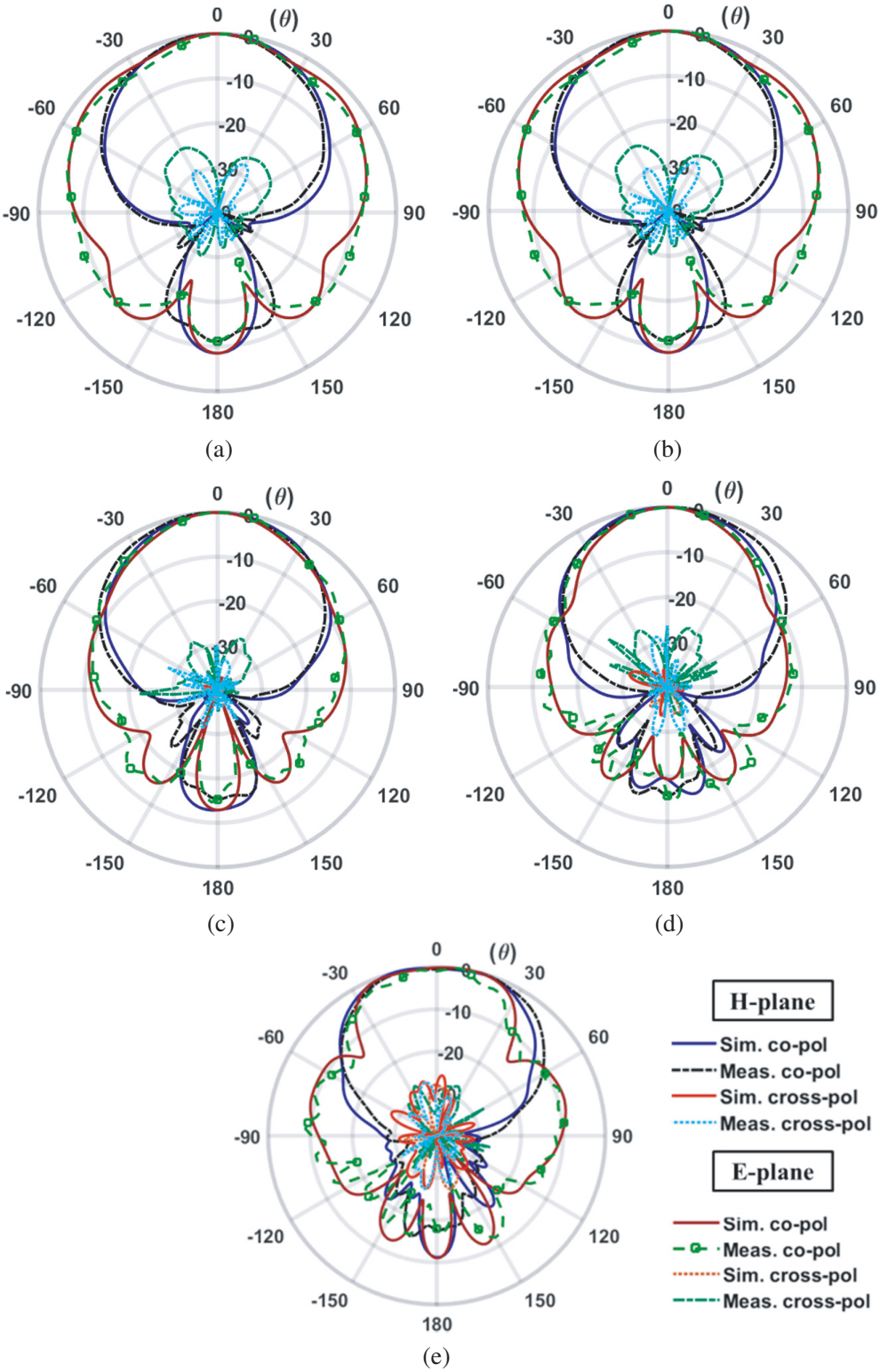

Figure 5. Measured and simulated co- and cross-pol patterns in the principal planes, when the antenna is excited in the SUM mode at (a) 3.5 GHz, (b) 4 GHz, (c) 4.6 GHz, (d) 5.1 GHz, (e) 5.7 GHz.

bandwidth range of $\sim 39\%$. The shorting posts along with the appropriately dimensioned V-slots aid in pushing the operating frequencies of the antenna towards the lower frequencies, away from the TM_{12} mode, which help in reducing the SLLs over a wide frequency range. Such a wide bandwidth range with no SLLs makes the proposed antenna an excellent candidate for high gain monopulse radar applications.

By changing the phase-shift between the probes from 180° to 0° using a 180° hybrid coupler, the antenna is set to operate in the DIFFERENCE mode with conical radiation patterns. Fig. 6 depicts the measured and simulated radiation patterns at 3.5, 4.6 and 5.7 GHz along the *XZ* and *YZ* planes. Good agreement between the simulated and measured radiation patterns is observed. Moreover, the realized conical radiation patterns are quite symmetric with a respectable null depth.

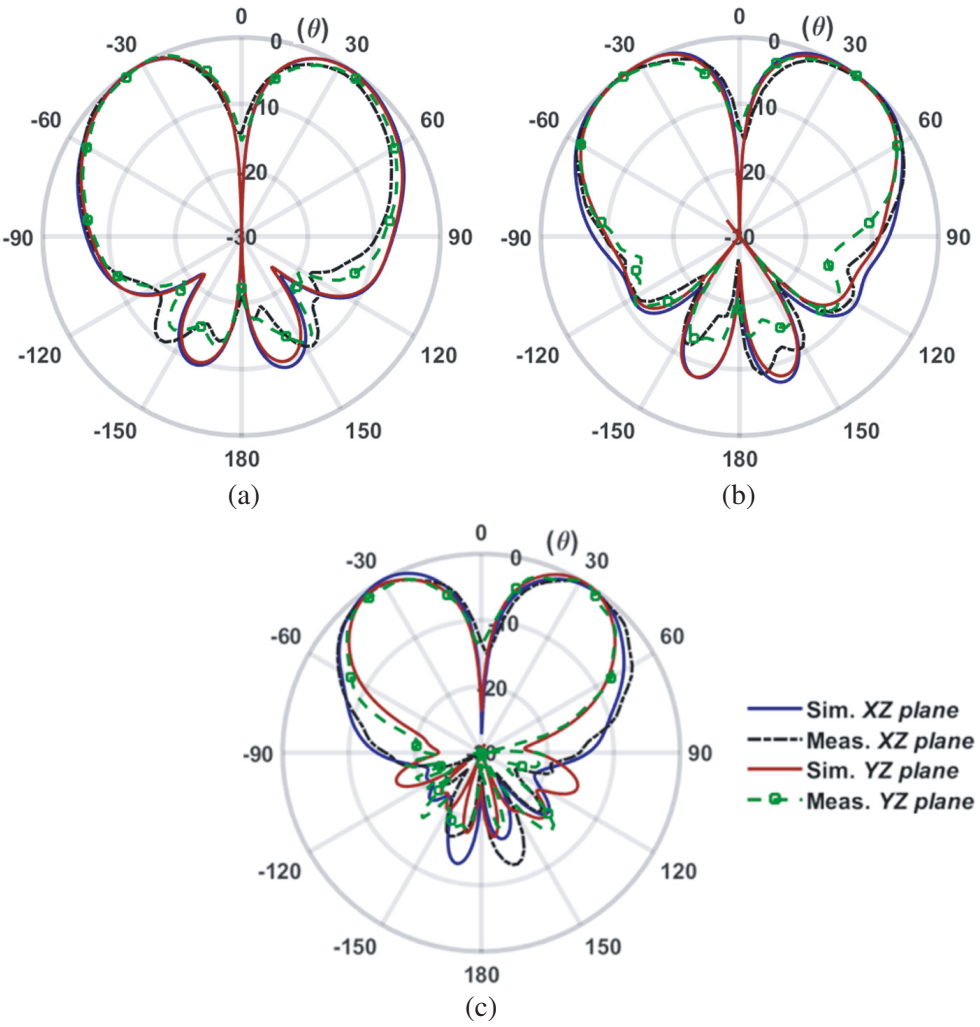

Figure 6. Measured and simulated DIFFERENCE patterns in the principal *XZ* and *YZ* planes at (a) 3.5 GHz, (b) 4.6 GHz, (c) 5.7 GHz.

To illustrate the 3-dB gain bandwidth of the SUM and DIFFERENCE modes, the peak gain is plotted versus frequency in Fig. 7 for both the modes. As observed, the gain variation is within the 3 dB limit over the entire frequency range, thus realizing a $\sim 48\%$ shared 3-dB gain bandwidth with the peak gain of ~ 11 dBi and ~ 8.2 dBi in the dominant and conical modes, respectively. There is a slight gain drop in the dominant TM_{11} mode at the high-end frequencies, which is attributed to the partial excitation of the next higher order broadside TM_{12} mode, as shown in Fig. 5(e). For reference, photographs of the fabricated antenna and the prototype antenna under test are embedded into Fig. 7.

To attain high gain characteristics for monopulse tracking applications, the designed antenna is

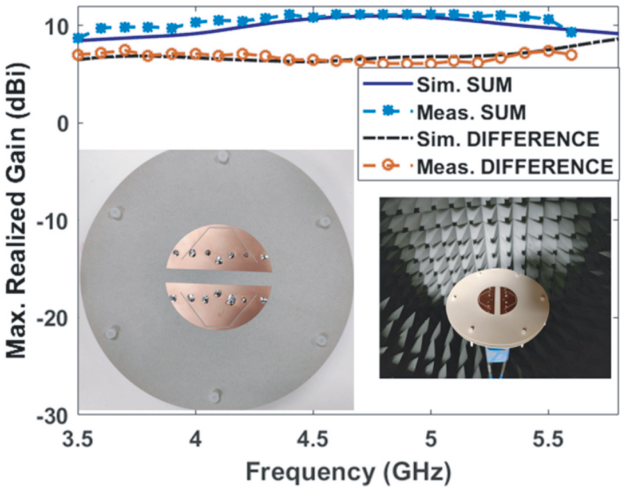

Figure 7. Frequency response of measured and simulated peak gain for SUM and DIFFERENCE modes along with the photographs of the fabricated antenna.

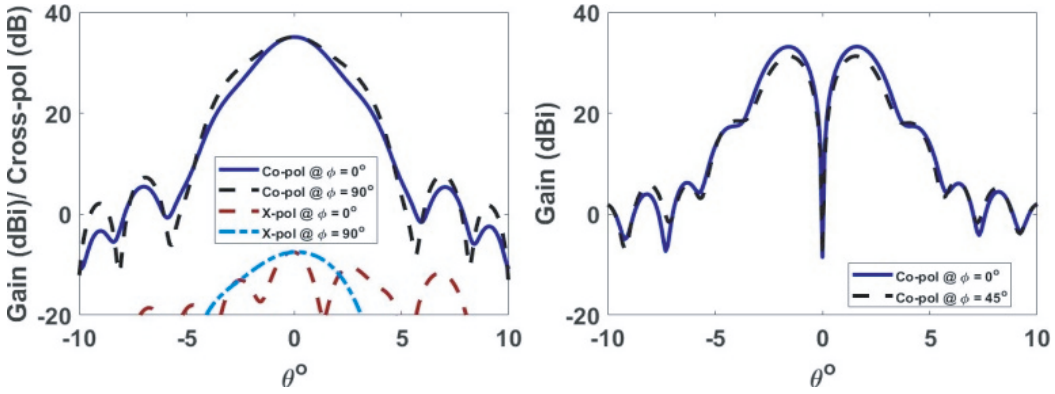

Figure 8. Secondary radiation patterns of the reflector antenna illuminated by the proposed patch antenna as a primary feed in the principal planes at 4.6 GHz. (a) Broadside mode. (b) Conical mode.

Table 2. Performance comparison of the proposed antenna with pertinent single-patch art works.

Ref. []	Single Patch	Height (λ_o)	Shared BW	SLL-free BW	Peak Gain (broadside/conical) (dBi)
[12]	✓	~ 0.12	$\sim 31\%$	$\sim 13\%$	$\sim 9/\sim 4$
[13]	✓	~ 0.07	$\sim 20\%$	$\sim 20\%$	$\sim 9.1/\sim 4.3$
[14]	✓	~ 0.06	$\sim 20\%$	$\sim 20\%$	$\sim 8.1/\sim 3.7$
[17]	✓	~ 0.12	$\sim 24\%$	$< 6\%$	$\sim 8.5/\sim 4$
[18]	✓	~ 0.2	$\sim 45\%$	$\sim 24\%$	$\sim 10.3/\sim 5.1$
[19]	✓	~ 0.07	$\sim 45\%$	$\sim 11\%$	$\sim 11.5/\sim 7.3$
Proposed Antenna	✓	$\mathbf{\sim 0.08}$	$\mathbf{\sim 48\%}$	$\mathbf{\sim 39\%}$	$\mathbf{\sim 11/\sim 8.2}$

numerically studied by placing it at the focal point of a parabolic reflector antenna. The diameter of the projected aperture of the parabolic dish is $30\lambda_o$, where λ_o is the free-space wavelength at 4.6 GHz. The focal length-to-diameter ratio is 0.375. The broadside and conical secondary radiation patterns of the reflector antenna at the center frequency of 4.6 GHz are shown in Fig. 8. They are symmetric and have almost equal beamwidths in the principal planes. The peak gain of the secondary broadside and conical radiation patterns is in the order of 37 dBi and 34 dBi, respectively.

Table 2 compares the characteristics of the proposed antenna with those of the reported wideband pattern diversity antennas in the literature with a single patch. As demonstrated, at the comparable height, the proposed design excels the other antennas in terms of its SLL-free bandwidth as well as the radiation characteristics.

5. CONCLUSION

A V-slotted T-probe fed circular patch antenna with wideband pattern diversity characteristics was proposed, investigated and validated in this article. The achieved active reflection coefficients for both the broadside and conical modes of operation were in the range of 48% from 3.5 to 5.7 GHz. More importantly, the SLL-free bandwidth was around 39% from 3.5 to 5.2 GHz. The realized reconfigurable radiation patterns were stable and symmetric throughout the operating frequency range. A respected null-depth of -25 dB was obtained over such a wide frequency range, thus making the antenna suitable for wireless communication and monopulse radar applications. Moreover, the experimental results matched well with the numerical antenna characteristics.

ACKNOWLEDGMENT

This work was supported in part by the National Science Foundation (NSF) CAREER Award No. ECCS-1653915.

REFERENCES

1. Dietrich, C. B., K. Dietze, J. R. Nealy, and W. L. Stutzman, "Spatial, polarization, and pattern diversity for wireless handheld terminals," *IEEE Trans. Antennas Propag.*, Vol. 49, No. 9, 1271–1281, Sept. 2001.
2. Sherman, S. M., *Monopulse Principles and Techniques*, 2nd Edition, Artech House, Norwood, MA, 2011.
3. Jiang, X., Z. Zhang, Y. Li, and Z. Feng, "A novel null scanning antenna using even and odd modes of a shorted patch," *IEEE Trans. Antennas Propag.*, Vol. 62, No. 4, 1903–1909, Apr. 2014.
4. Lawrence, N. P., C. Fumeaux, and D. Abbott, "Planar triorthogonal diversity slot antenna," *IEEE Trans. Antennas Propag.*, Vol. 65, No. 3, 1416–1421, Mar. 2017.
5. Saurav, K., N. K. Mallat, and Y. M. M. Antar, "A three-port polarization and pattern diversity ring antenna," *IEEE Antennas Wireless Propag.*, Vol. 17, No. 7, 1324–1328, Jul. 2018.
6. Krishnamoorthy, K., B. Majumder, J. Mukherjee, and K. P. Ray, "Low profile pattern diversity antenna using quarter-mode substrate integrated waveguide," *Progress In Electromagnetics Research Letters*, Vol. 55, 105–111, 2015.
7. Zheng, Y., G. A. E. Vandenbosch, and S. Yan, "Low-profile broadband antenna with pattern diversity," *IEEE Antennas Wireless Propag.*, Vol. 19, No. 7, 1231–1235, Jul. 2020.
8. Sun, L., W. Huang, B. Sun, Q. Sun, and J. Fan, "Two-port pattern diversity antenna for 3G and 4G MIMO indoor applications," *IEEE Antennas Wireless Propag.*, Vol. 13, 1573–1576, Aug. 2014.
9. Lin, W., H. Wong, and R. W. Ziolkowski, "Wideband pattern-reconfigurable antenna with switchable broadside and conical beams," *IEEE Antennas Wireless Propag.*, Vol. 16, 2638–2641, Aug. 2017.
10. Yang, X., H. Lin, H. Gu, L. Ge, and X. Zeng, "Broadband pattern diversity patch antenna with switchable feeding network," *IEEE Access*, Vol. 6, 69612–69619, Oct. 2018.

11. Lin, W., H. Wong, and R. W. Ziolkowski, "Circularly polarized antenna with reconfigurable broadside and conical beams facilitated by a mode switchable feed network," *IEEE Trans. Antennas Propag.*, Vol. 66, No. 2, 996–1001, Feb. 2018.
12. Deng, C., X. Lv, and Z. Feng, "Wideband dual-mode patch antenna with compact CPW feeding network for pattern diversity application," *IEEE Trans. Antennas Propag.*, Vol. 66, No. 5, 2628–2633, May 2018.
13. Wei, K., Z. Zhang, W. Chen, and Z. Feng, "A novel hybrid-fed patch antenna with pattern diversity," *IEEE Antennas Wireless Propag.*, Vol. 9, 562–565, May 2010.
14. Liu, J., Z. Weng, Z.-Q. Zhang, Y. Qiu, Y.-X. Zhang, and Y.-C. Jiao, "A wideband pattern diversity antenna with a low profile based on metasurface," *IEEE Antennas Wireless Propag.*, Vol. 20, No. 3, 303–307, Mar. 2021.
15. Sun, L., G. Zhang, B. Sun, W. Tang, and J. Yuan, "A single patch antenna with broadside and conical radiation patterns for 3G/4G pattern diversity," *IEEE Antennas Wireless Propag.*, Vol. 15, 433–436, Jun. 2015.
16. Cui, L., W. Wu, and D. Fang, "Wideband circular patch antenna for pattern diversity application," *IEEE Antennas Wireless Propag.*, Vol. 14, 1298–1301, Feb. 2015.
17. Yang, S. L. S. and K. M. Luk, "Design of a wide-band L-probe patch antenna for pattern reconfiguration or diversity applications," *IEEE Trans. Antennas Propag.*, Vol. 54, No. 2, 433–438, Feb. 2006.
18. Toh, W. K., Z. N. Chen, X. Qing, and T. S. P. See, "A planar UWB diversity antenna," *IEEE Trans. Antennas Propag.*, Vol. 57, No. 11, 3467–3473, Nov. 2009.
19. Radavaram, S. and M. Pour, "Reply to comments on "Wideband radiation reconfigurable microstrip patch antenna loaded with two inverted U-slots"," *IEEE Trans. Antennas Propag.*, Vol. 68, No. 2, 1216–1218, Feb. 2020.
20. Rafi, G. Z. and L. Shafai, "Wideband V-slotted diamond-shaped microstrip patch antenna," *Electron. Lett.*, Vol. 40, No. 19, 1166–1167, Sept. 2004.
21. Rafi, G. and L. Shafai, "Broadband microstrip patch antenna with V-slot," *IEE Proc. — Microwaves, Antennas Propag.*, Vol. 151, No. 5, 435–440, Oct. 2004.
22. Elsadek, H. and D. M. Nashaat, "Multiband and UWB V-shaped antenna configuration for wireless communications applications," *IEEE Antennas Wireless Propag. Lett.*, Vol. 7, 89–91, May 2008.
23. Wong, H., K. K. So, and X. Gao, "Bandwidth enhancement of a monopolar patch antenna with V-shaped slot for car-to-car and WLAN communications," *IEEE Trans. Vehicular Technology*, Vol. 65, No. 3, 1130–1136, Mar. 2016.
24. Qu, S. and Q. Xue, "A Y-shaped stub proximity coupled V-slot microstrip patch antenna," *IEEE Antennas Wireless Propag. Lett.*, Vol. 6, 40–42, Mar. 2007.
25. High Frequency Structure Simulator (HFSS 19.0), ANSYS, Canonsburg, PA, Boston, MA.
26. Weigand, S., G. H. Huff, K. H. Pan, and J. T. Bernhard, "Analysis and design of broad-band single-layer rectangular U-slot microstrip patch antennas," *IEEE Trans. Antennas Propag.*, Vol. 51, No. 3, 457–468, Mar. 2003.
27. Lam, K. Y., K. Luk, K. F. Lee, H. Wong, and K. B. Ng, "Small circularly polarized U-slot wideband patch antenna," *IEEE Antennas Wireless Propag. Lett.*, Vol. 10, 87–90, Feb. 2011.
28. Radavaram, S. and M. Pour, "Wideband radiation reconfigurable microstrip patch antenna loaded with two inverted U-slots," *IEEE Trans. Antennas Propag.*, Vol. 67, No. 3, 1501–1508, Mar. 2019.